

Pair condensation and inter-layer coupling in cuprates: pairing on a superlattice

P. Süle

Research Institute for Technical Physics and Material Science,
Konkoly Thege u. 29-33, Budapest, Hungary,
sule@mfa.kfki.hu
(January 30, 2020)

We analyze the superconducting state and c -axis charge dynamics of cuprates using a charge ordered bilayer superlattice model in which pairing is supported by inter-layer Coulomb energy gain (potential energy driven superconductivity). The superlattice nature of high- T_c superconductivity is experimentally suggested by the smallness of the in-plane coherence length $\xi_{ab} \approx 10 - 30\text{\AA}$ which is comparable with a width of a 4×4 to 8×8 square supercell lattice layer. The $2D \Leftrightarrow 3D$ quantum phase transition of the hole-content at T_c , supported by c -axis optical measurements, is also studied. The pair condensation might lead to the sharp decrease of the normal state c -axis anisotropy of the hole content and hence to the decrease of inter-layer dielectric screening. The drop of the c -axis dielectric screening can be the primary source of the condensation energy below T_c . We find that a net gain in the electrostatic energy occurs along the c -axis, which is proportional to the condensation energy: $E_c^{3D} \approx E_{cond}$ and is due to inter-layer charge complementarity (charge asymmetry of the boson condensate). The bilayer model naturally leads to the effective mass of $m^* \approx 4m_e$ found by experiment. The static c -axis dielectric constant ϵ_c is calculated for various cuprates and compared with the available experimental data. We find correlation between T_c and the inter-layer spacing d , ϵ_c and the coherence area of the condensate. The 2D pair-condensate can be characterized by a charge ordered state with a "checkboard" like pattern seen by scanning tunneling microscopy.

I. INTRODUCTION

It is more or less generally accepted now that the conventional electron-phonon pairing mechanism cannot explain cuprate superconductivity, because as high a transition temperature as $164K$ cannot be explained by the energy scale of lattice vibrations without leading to lattice instability [1]. It is already well established that much of the physics related to high-temperature superconductivity (HTSC) is in 2D nature, one of the basic questions to be answered, however, in the future is whether HTSC is a strictly 2D phenomenon or should also be described by a 3D theory. A well known experimental fact is that the zero resistance occurs along the ab plane and the c -axis at the same critical temperature [2] suggesting that there must be inter-layer (IL) coupling involved in the mechanism which drives the system into HTSC. Another experiment, such as the intercalation on Bi2212 [3], however leads to the opposite conclusion. Intercalation of I or organic molecules, which expands the unit cell significantly along the c -axis, does not affect T_c . This finding is against IL coupling and supports low-dimensional theories. The large anisotropy of the resistivity (and of other transport properties) is again not in favour of 3D theories of HTSC [2]. Moreover, Basov *et al.* reported c -axis optical results and detected a small lowering of kinetic energy in the IL transport of cuprates [4]. This finding again indicates the importance of IL coupling in high temperature superconductors. There are a couple of other findings against and supporting the 3D nature of HTSC [5–7]. Most notably the systematic dependence of the transition temperature T_c on the c -axis structure and, in particular, on the number of CuO_2 planes in mul-

tilayer blocks also strongly in favour of the 3D character of HTSC. It is therefore, a fundamental question whether at least a weak IL coupling is needed for driving the system to a superconducting (SC) state or a single CuO_2 layer is sufficient for superconductivity [8].

There has been considerable effort spent on understanding HTSC within the context of IL coupling mechanism in the last decades in which c -axis energy is available as a pairing mechanism [9–12]. In other approaches the importance of IL hopping is emphasized *vs.* the direct IL Coulomb interaction of charged sheets [5,8]. There is another theory providing explanation for HTSC using the general framework of BCS combined with IL coupling [13]. The so-called IL tunnelling (ILT) theory [5,8], however, is no longer considered a viable mechanism for SC in cuprates since ILT could provide no more than 1% of the condensation energy in certain cuprates [1,6,14].

Recently, optical data have been reported for Bi2212 [15], which supports the quantitative predictions of Hirsch [16], in which the carriers lower their kinetic energy upon pair formation (kinetic-energy-driven superconductors) and hence this is the largest contribution to the condensation energy. Anyhow, the role of direct IL Coulomb interaction is still not ruled out as a possible explanation for HTSC, especially if we take into account that no widely accepted theory is available until now which accounts for the apparent 3D nature of HTSC [5,6].

In this paper we propose a simple phenomenological model for explaining the 3D character of HTSC in cuprates supported by calculations. We would like to study the magnitude of direct Coulomb interaction between charge ordered square superlattice layers as a pos-

sible source of pairing interaction. Our intention is to understand HTSC within the context of an IL Coulomb-mediated mechanism. Of particular relevance to our investigation are the doping, multilayer, and pressure dependence of T_c in terms of a charge ordered *superlattice nature* of pair condensation, which is often neglected in the past. On the other hand the size of a characteristic superlattice can directly be related to the in-plane coherence length ξ_{ab} of cuprates, which is proportional to the linear size of the pair condensate (real space pairing) of the superconducting island in the ab -plane [17]. The IL charging energy we wish to calculate would then depend on the IL spacing (d), the IL dielectric constant ϵ_c , the hole content n_h and the size of the superlattice. A large body of experimental data are collected which support our model. Finally we calculate the static c -axis dielectric constant ϵ_c for various cuprates which are compared with the available experimental observations.

It is commonly accepted that charge carriers are mainly confined to the 2D CuO_2 layers and their concentration is strongly influenced by the doping agent via hole doping (both by chemical and field effect doping [18]). Holes (no charge and spin at a lattice site) in the 2D CuO_2 layers are the key superconducting elements in high temperature superconductivity (HTSC). A characteristic feature of many high temperature superconductors (HTSCs) is the optimal hole content value of $n_h \approx 0.16e$ per CuO_2 layer at optimal doping in the normal state (NS) [19]. *Our starting hypothesis is that the hole content goes through a reversible $2D \leftrightarrow 3D$ quantum phase transition at T_c in layered copper oxides.* Optical studies on the c -axis charge dynamics reveals this phenomenon: the c -axis reflectance is nearly insulating in the NS but below T_c is dominated by the Josephson-like plasma edge [4]. Below T_c a sharp reflectivity edge is found at very low frequencies (lower then the superconducting gap) for a variety of cuprates arising from the carriers condensed in the SC state to the ab -plane and from the onset of coherent charge transport along the c -axis [20–24]. Band structure calculations predict an appreciable c -axis dispersion of bands close to the Fermi surface and thus an anisotropic three-dimensional metallic state [25]. Other first principles calculations indicate that above T_c the hole charge n_h is charge transferred to the doping site ($2D \rightarrow 3D$ transition) [26,27]. Furthermore, we expect that below T_c the hole-content condenses to the sheets forming *anti-hole regions* (hole-content charge at a lattice site, $3D \rightarrow 2D$ transition). An anti-hole corresponds to an excess charge condensed to a hole lattice site in the sheet below T_c . Therefore, in the normal state hole doping is the dominant charge transfer mechanism while in the superconducting (SC) state the opposite is true: the IL hole-charge is transferred back to the CuO_2 planes (charging of the sheets). The latter mechanism can be seen by the measurement of transport properties as a function of temperature [2,28–30] if we assume that the increase in the density of in-plane free carriers below T_c is due to pair condensation. The sharp temperature

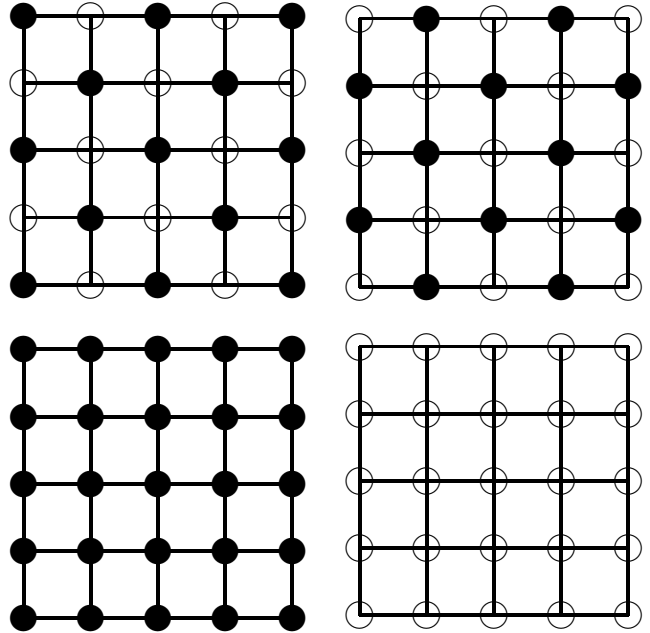


FIG. 1. Upper panels: The charge ordered state of the type of a "checkerboard" of the hole-anti-hole condensate. Opened and filled circles denote the holes with a charge of $q_i = +0.16e$ and anti-holes ($q_j = -0.16e$), respectively in the 5×5 square lattice layer model. Note that the left panel accommodates 13 anti-holes which corresponds to $2e + 0.16e$ charge,. The right panel contains 12 anti-holes corresponding to $2e - 0.16e$ charge. The two lower panels correspond to the antiferromagnetic insulating state (left) and to the holed-doped system (normal state, right).

dependence of the c -axis dielectric constant ϵ_c and optical conductivity [31] seen in many cuprates and in other perovskite materials also raises the possibility of a $2D \leftrightarrow 3D$ condensation mechanism at T_c [2,32]. Therefore, the pair condensation can be described by an anisotropic 3D condensation mechanism, and by a doping induced 2D-3D dimensional crossover [7].

In any naive model of electron pairing in cuprates the Coulomb repulsion is troublesome. When the pairs of charged carriers are confined to the 2D sheets, naturally a net self-repulsion of the pair condensate occurs. Although short-range Coulomb screening in the dielectric crystal can reduce the magnitude of the repulsion but it is insufficient to cancel Coulomb repulsion [33]. Spatial separation should reduce the interaction strength, but even at 14\AA $e^2/r \approx 1\text{eV}$ if unscreened. One can assume capacitative effect between the CuO_2 planes: The charged boson condensate in one plane is stabilized by a deficiency of that charge on another plane [33]. The various forms of the capacitor model are associated with the 3D character of HTSC, considering the inter-layer charge reservoir as a dielectric medium [33]. The inter-

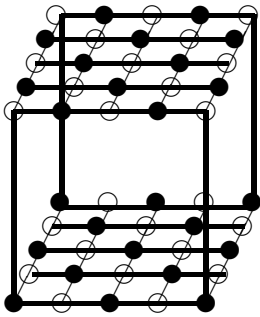


FIG. 2. The charge ordered state of the hole-anti-hole condensate in the bilayer 5×5 superlattice model. Note the charge asymmetry between the adjacent layers. The bilayer can accommodate a pair of boson condensate ($4e$)

layer charging energy might be insufficient to stabilize the self-repulsion of the holes in one plane and the self-repulsion of the charge condensate on another plane in the capacitor model. Also, the superconducting properties of the hole-rich and nearly hole-free sheets would be different which is not verified by experimental techniques.

Our intention is to combine the 2D and 3D nature of HTSC. Therefore, we propose a phenomenological model in which the charge distribution of the planes is polarized in such a way that holes and anti-holes (hole-electron pair) are phase separated within each of the sheets leading to a charge ordered state. We also study the magnitude of IL coupling (direct IL Coulomb interaction) between 2D charge ordered superlattices.

Charging of the sheets: The CuO_2 layers carry negative charge obtained from the charge reservoir even in the insulating stoichiometric materials, e.g. in the infinite layer compound $CaCuO_2$ each layer is charged by $2e$ charge donated by the Ca atoms. In $(CuO_2)^{2-}$ then the electron configuration of Cu and O is $3d^{10}4s^1$ and $2p_z^2$. Unit $(CuO_2)^{2-}$ is typical of any undoped (stoichiometric) cuprates and *ab initio* calculations provide approximately the charge state $Cu^{1.5+}O_2^{3.5-}$ [2,25] which is due to charge redistribution between Cu and O. The $(CuO_2)^{2-}$ plane itself is antiferromagnetic and insulating, e.g. there are no holes in the "overcharged" layers. Upon e.g. Oxygen doping, however, the doping charge n_h is transferred along the c -axis to the doping site, since the doping atom exhibits a rare gas electron structure (O^{2-}) [26,27].

Our basic assumption is that in the SC state every second hole with the charge of $+n_h$ is filled up by the doping charge n_h due to the *condensation* of the hole-content n_h to the sheets. The electrostatic field of the doping site or the external field of the field-effect transistor *confines* [18] the anisotropic hole-content to the *anti-hole* sites of the sheet leading to a charge ordered state (FIG. 1) below T_c . Briefly, the c -axis anisotropy of the hole content is strongly temperature dependent in cuprates. *The phase separation of the holes and anti-holes (leading to a charge*

ordered state) is stabilized by the intra- and inter-layer hole-anti-hole interactions. Basically the phase separation of holes and anti-holes in the planes is the manifestation of strong Coulomb correlation in the SC state. The Coulomb repulsion arising within the anti-hole sites is suppressed by the hole-anti-hole interactions.

II. THE SUPERLATTICE MODEL

We propose to examine the following superlattice model of pair condensation: A pair of charge carriers ($2e$) is distributed over $2/0.16 = 12.5$ CuO_2 unit cells in a square lattice layer if the $2e$ pair is composed of the hole charge $n_h \approx 0.16/CuO_2$. However, allowing the phase separation of hole-anti-hole pairs, every second unit cell is occupied by $-0.16e$ (anti-hole), and the rest is empty (holes, $+0.16e$), therefore we have 25 unit cells for a condensed pair of charge carriers (Fig 1., that is the unit lattice of the pair condensate in the 5×5 supercell model). Therefore, $2n_h = -0.32e$ hole charge condenses to every second hole forming anti-hole sites. The remarkable feature is that the size of the 5×5 condensate (four lattice spacings, $4a \approx 15.5\text{\AA}$) is comparable with the measured small coherence length ξ_{ab} of single-layer cuprates ($\xi_{ab} \sim 10\text{\AA}$ to 20\AA) [2,17,34,35]. ξ_{ab} can directly be related to the characteristic size of the wave-packet of the Cooper pair (coherence area) [2,17]. The supercell model can be applied not only for $n_h = 0.16e$ but also for the entire doping regime. Our expectation is that the charge ordered state of the 5×5 model given in Fig. 1 can be an effective model state for describing the SC state. An important feature of this model is the *charge separation* dq in the charge ordered state, where $+0.16e$ and $-0.16e$ partial boson charges are localized alternatively ($dq = 0.32e$). The hopping of a partial charge from the anti-hole sites to the holes can reduce the magnitude of the charge separation dq leading to the extreme case when $dq = 0$ which is nothing else than the $(CuO_2)^{2-}$ antiferromagnetic insulating state. Therefore characteristic quantity of the SC state dq is directly related to the hole-content seen in cuprates in the NS as a function of doping.

The hopping of anti-holes in such a charge ordered lattice layer might lead to SC without considering any lattice vibration effects when dq is in the optimal regime. Due to the charge redistribution mentioned above net repulsion occurs between the portions of the $2e$ charge within different sites in the SC state (intra CuO_2 repulsion), and attraction occurs between the adjacent CuO_2 units with opposite charges (inter $0.16 - \dots - 0.16 +$ interaction). Also, charging energy gain occurs out-of-plane due to inter-layer attraction (E_{el}^c). Below T_c the charge-ordered state becomes stable compared with the competing phase of the NS supported by IL charging energy. Holes and anti-holes are placed in such a way in adjacent layers to maximize E_{el}^c . Therefore, holes in one of the

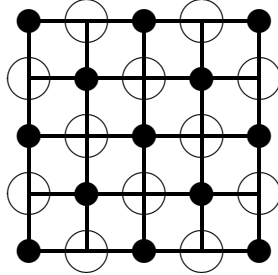


FIG. 3. The charge ordered state of the normal state. Opened and filled circles denote the holes with a charge of $q_i \approx +0.32e$ and anti-holes ($q_j \approx -0.16e$), respectively in the 5×5 square lattice layer model.

layers are always covered by anti-holes in the other layer and *vice versa* (FIG. 2, inter-layer *electrostatic complementarity*, bilayer 5×5 model). An important feature is then that the boson condensate can be described by an inter-layer *charge asymmetry*. The IL coupling of boson-boson pairs in the bilayer 5×5 model naturally suggests the effective mass of charge carriers $m^* \approx 4m_e$, as it was found by measurements [36,39]. Notable feature of the antisymmetric 5×5 bilayer model is that the basal plane contains 13 anti-holes and 12 holes while the reverse is true for the adjacent layer: it contains 12 anti-holes and 13 holes (FIG. 2).

The following charging model systems can be considered:

(1) *purely hole-doped model*: In each sheet each CuO_2 units possese $n_h = +0.16e$ charge. The hole charge n_h is charge transfered to the charge reservoir (doping site). In this model one can naively expect that the self-repulsion of a hole rich sheet can be quite large. In order to reduce the hole-hole self-repulsion of the sheets, a hopping of $\sim n_h$ between the adjacent hole sites would result in the reduction of the repulsion. As is well known, the hopping of certain amount of charge ($\sim n_h$) between the holes leads to metallic conductance which is typical of hole-doped cuprates (FIG. 3). Strong Coulomb forces also arise between the negatively charged doping site and the positive sheets. This interaction may well stabilize the system. This is the *normal state* (NS) of the cuprates. Due to the strong *c*-axis anisotropy of the hole charge in the NS IL dielectric screening is large in this state because of the increase in the dynamic component of the IL dielectric permittivity (ϵ_c).

(2) *charged sheet model*: Each of the superconducting sheets (CuO_2^{2-}) and the charge reservoir in its doping site are charged. According to *ab initio* calculations [27], the doping oxygen in Hg1201 can get the excess negative charge either from the charge reservoir or from the planes. The doping charge or the external field polarizes the diffuse charge distribution of the sheets. In this way holes and anti-holes occur in the planes which leads to inter-layer charging energy. In the sheets *charge patterns* can be formed, e.g. hole-rich and anti-hole rich regions.

Within this model $\pm 0.16e$ charges/ CuO_2 are placed alternatively in the lattice ($dq = 0.32e$). The pair-binding energy is provided by the self-interaction of the charge-ordered condensate at low temperature. However, our proposal is to understand HTSC in such a way that the pair-condensate is stabilized at higher temperature by the IL-charging energy provided by the antisymmetry of the pair-condensate charge density between the adjacent layers.

The *c*-axis dielectric constant of the SC state is reduced to the average value of the IL dielectric medium due to the pair condensation of the hole charge to the sheets. No IL screening of the hole charge occurs in this state which may well lead to energy gain and hence Coulomb induced pairing in the sheets. Our proposal is that when the system goes to SC state, the conduction band loses its 3D anisotropy due to the 2D pair-condensation of the hole-content which leads to resistivity-free hole-conductivity in the planes below T_c .

III. THE TOTAL ENERGY OF THE PAIR CONDENSATE

Those who believe that high- T_c Cooper pairing can be attributed to Coulomb forces would agree that the key ingredient in this expression is the energy- and momentum-dependent dielectric function ϵ_c of the solid. Our intention is to develop a simple working hypothesis in which the IL charge reservoir provides an average dielectric background and the hole content further enhances IL dielectric screening when $2D \rightarrow 3D$ transition occurs (hole-doping, the NS). The dielectric plasma provided by the hole charge results in the dynamic screening effect of Coulomb interaction which is typical of hole doped cuprates in the NS. In the opposite case ($3D \rightarrow 2D$, pair condensation) the IL dielectric screening is nearly reduced to the average background value of the IL ion core spacer. This is what leads to IL energy gain. The underlying source of the condensation energy is then the energy gain due to the lack of dynamic screening in the SC state. The possibility of direct IL hopping of Cooper pairs is not considered within this model as it was ruled out as important aspect of HTSC [6].

We start from a very general description of our model system using e.g. a Hamiltonian similar to that is given elsewhere [10] or which can also partly be seen in general text books [40]. We would like to describe then the $2D \leftrightarrow 3D$ condensation of the hole-content using the Hamiltonian

$$H = \sum_i H_i^{2D} + \sum_{i,j} H_{ij}^{3D}, \quad (1)$$

where H_i^{2D} is the BCS-type Hamiltonian of the intra-layer condensate.

$$H_i^{2D} = \sum_{k,\sigma} \epsilon_k c_{k\sigma,i}^\dagger c_{k\sigma,i} \quad (2)$$

$$+V \sum_{k,k'} c_{k\uparrow,i}^\dagger c_{-k\downarrow,i}^\dagger c_{k\downarrow,i} c_{-k\uparrow,i}.$$

In Eq. (2) $c_{k\uparrow,i}^\dagger$ is the creation operator for electrons in the i th layer, with linear momentum \mathbf{k} within the layer and spin σ , using the effective-mass approximation $\epsilon_k = \hbar^2 k^2 / 2m^*$. $V = -|V|$ is the attractive inter-layer interaction (3D coupling) and is assumed to originate from some of the proposed mechanisms [5,9–11]. The attractive IL term H_{ij}^{3D} given by

$$H_{ij}^{3D} = -t \sum_{k\sigma,\alpha,\beta} c_{k\sigma,i}^\dagger c_{k\sigma,j} + Y \sum_{k,k'} c_{k\alpha,i}^\dagger c_{-k\beta,j}^\dagger c_{-k\beta,j} c_{k\alpha,i} + W \sum_{k,k',\alpha,\beta} c_{k\alpha,i}^\dagger c_{-k\beta,i}^\dagger c_{-k\beta,i} c_{k\alpha,j}. \quad (3)$$

The first term in Eq. (3) is the direct IL hopping, while the second and third terms describe IL coupling in a general form. t is very small in oxide superconductors [6,10]. Y denotes the IL coupling assisted by direct Coulomb interaction between charged layers (this is of particular interest in our model). W is the coupling constant and can arise through the Coulomb interaction causing inter-band transitions at the Fermi surface to some of the occupied or empty bands away from the Fermi level, with finite dispersion, however, along the c -axis. In this paper we consider only the second term in Eq. (3) as the source of the attractive interaction for pairing and neglect the rest of the inter-layer Hamiltonian H_{ij}^{3D} ($t \approx 0, W \approx 0$).

We calculate then the energy of the nearly 2D electron pair condensate in the CuO_2 plane for the bilayer supercell problem. It is assumed that the pair condensate behaves as a nearly free electron gas with ab -kinetic energy E_{kin}^{ab} and potential energy, which is mainly its in-plane self-electrostatic energy (E_{el}^{ab}) and the out-of-plane inter-layer interaction energy (E_{el}^c). For simplicity, the rest of the electron system is neglected completely. The external potential of the condensate is also excluded in this model, that is the lattice-condensate interaction, which is assumed to be negligible in the charged (CuO_2)²⁻ system (at least its contribution is negligible to the condensation energy). In other words the ionic background of the planes is screened by the core and valence electrons of the (CuO_2)²⁻ plane. The kinetic energy of the charge condensate is due to the hopping of the charge carriers between the CuO_2 sites within the sheets. We do not take into account the complications due to ionic heterogeneity, nonpointlike polarization, etc. The effective Coulomb interaction between spinless point-charges may be approximated by the expression $V_{eff}(\mathbf{r}) = e^2 / (4\pi\epsilon_0\epsilon_c\mathbf{r})$, where ϵ_c takes into account phenomenologically the dielectric screening effect of the IL dielectric medium and confined hole charge. This kind of a rough approximation has widely used by several groups in the last decade [9,33,36,52]. The important feature is that the c -axis dielectric screening (ϵ_c) is nearly reduced to the static value of the average background dielectric constant in the SC

state. In accordance with this a sharp temperature dependence of $\epsilon_c(\omega)$ is found in BSCCO by c -axis optical measurements at T_c [31]. The static out-of-plane dielectric function can be obtained from the sum rule

$$\epsilon_c = \epsilon_1(0) + \frac{2}{\pi} \int_0^\infty \frac{\epsilon_2(\omega')}{\omega'} d\omega', \quad (4)$$

where $\epsilon_2(\omega)$ is the dynamic component of $\epsilon_c(\omega)$ [49].

Although, the r -dependence of the screened in-plane electrostatic interaction between the condensed charges q_i and q_j is not perfectly $1/r$, we approximate it with the expression $V_{eff}^{ab} \approx e^2 / 4\pi\epsilon_0\epsilon_{ab}r$ as well, where screening is taken into account implicitly via ϵ_{ab} . The lowest eigenvalue of H given in Eq. (1) is $E = \langle \Psi | H | \Psi \rangle$, where $\Psi(r_1, r_2) = \sum_k g(k) e^{i\vec{k} \cdot \vec{r}_1} e^{i\vec{k} \cdot \vec{r}_2}$ being the wavefunction of the interacting pair and $g(k)$ is a pair-correlation function [17]. Then the energy of the lowest eigenstate of the condensate in the SC state is approximated by using a pure dielectric form for the potential energy

$$E = E_{kin}^{ab} + E_{el}^{ab} + E_{el}^c = \frac{\hbar^2}{2m^*} \Delta\Psi(r_1, r_2) + \frac{e^2}{4\pi\epsilon_0} \left(\frac{1}{\epsilon_{ab}} \sum_{ij} \frac{q_i^{(1)} q_j^{(1)}}{r_{ij}^{(1)}} + \frac{1}{\epsilon_c} \sum_{n=1}^2 \sum_{m=2}^\infty \sum_{ij} \frac{q_i^{(n)} q_j^{(m)}}{r_{ij}^{(n,m)}} \right), \quad (5)$$

where \hbar is the Planck constant, $m^* \simeq 4m_e$ is the effective mass for the holes induced in the half-filled bands [36], n, m are layer indices, $r_{ij}^{(1)}$ and $r_{ij}^{(n,m)}$ are the intra-layer and inter-layer point charge distances, respectively. The most important components are the interactions with $r_{ij}^{(1,2)}$ (bilayer components), however one has to sum up for the IL interactions with terms $r_{ij}^{(n,m)}$, where $m = [2, \infty]$. Note that only the interactions of various layers with the basal bilayer (FIG. 2) are considered along the c -axis in both directions (up and down). The in-plane electrostatic screening ϵ_{ab} is completely separated from the out-of-plane dielectric screening (ϵ_c). q_i, q_j are the partial point charges/atoms in the $N \times N$ superlattice model at optimal doping.

$$q_{i,j} = \pm \frac{2N_h}{3N^2}, \quad (6)$$

where factor 2 is due to the fact that every second CuO_2 site is occupied by anti-holes, and each of them consists of 3 atoms ($q_{i,j} \approx \pm 0.053e$ at maximal charge separation). For the sake of simplicity it is assumed that the charges are equally distributed among Cu and O atoms within a CuO_2 site. The number of the lattice sites in the characteristic superlattice is N^2 and

$$\xi_{ab} \approx (N-1)a_0 \quad (7)$$

where $a_0 \approx 3.88\text{\AA}$ is ab lattice constant. $N_h = 2e$ is the charge of the electron pair. The anti-hole charges q_i^{hole}

must satisfy the *charge sume rule* within a characteristic bilayer over a coherence area $\sim \xi_{ab}^2$

$$\sum_{i=1}^{N^2} q_i^{a\text{hole}} = 4e, \quad (8)$$

where $q_i^{a\text{hole}}$ represents the anti-hole point charges. Naturally the charge neutrality $\sum_{ij}^{2N^2} (q_i^{hole} + q_j^{a\text{hole}}) = 0$ is also required. In this paper we study the lattice size $N \times N = 5$, which we found nearly optimal for a variety of cuprates. However, it can be interesting to study the variation of the "characteristic" lattice size in different cuprates as a function of various parameters (doping, pressure etc.). The kinetic energy of the boson condensate arises from the hopping of anti-holes (hole-anti-hole exchange) between the adjacent sites within the sheets, against the electrostatic background of the rest of the hole-anti-hole system. Single hole-anti-hole exchange is forbidden since extraordinary repulsion occurs which leads to the redistribution of the entire hole-anti-hole charge pattern. The collective intersite anti-hole hopping results in the kinetic energy of the condensate. If we chose appropriately the in-plane dielectric constant ($\epsilon_{ab} \approx 3.0$ [15,42]), we get the following result using Eq. (2):

$$E_{kin}^{ab} + E_{el}^{ab} \approx 0. \quad (9)$$

Consequently, no net in-plane energy gain is available for HTSC in this model. In other words we expect no role of pairing induced kinetic energy gain contrary to other theories [1,5,16] since the kinetic energy of the condensate is cancelled by the in-plane electrostatic energy. This is basically the manifestation of the virial theorem ($2T + V = 0$) for the *ab*-plane and is reasonable to expect its validity when weak IL coupling is assumed, where $E_{kin}^{ab} = 2T$ and $E_{el}^{ab} = V$. If the inter-sheet coupling is not that weak, then kinetic energy gain can occur in the planes (the violation of the in-plane virial theorem). It can therefore be the subject of further studies that both *ab*-plane kinetic energy and the screened *c*-axis IL Coulomb interaction can be the source of the condensation energy in the SC state. It is interesting that Eq. (9) holds when the measured mass enhancement of $m^* \approx 4m_e$ is used [36]. We can account for this mass enhancement if a pair of boson condensate charge $4e$ is distributed within the bilayer $N \times N$ model. The basic question is whether the pair condensation ($3D \rightarrow 2D$ transition of the hole charge) changes the kinetic energy or not in cuprates, however, is not well understood yet. For the sake of simplicity we neglect here the role of kinetic energy lowering and employ Eq. (9) as it stands.

Taking the energy difference $\Delta E_{tot} = |E_{tot}^{NS} - E_{tot}^{SC}|$, the energy gain in the SC state (condensation energy) can be given as follows,

$$E_{cond} \approx \Delta E_{el}^c = |E_{el}^{c,NS} - E_{el}^{c,SC}|. \quad (10)$$

The NS contribution to Eq. (10) is $E_{el}^{c,NS} \approx 0$, if IL coupling is screened effectively (large density of the hole content in the IL space \sim large $\epsilon_c(NS)$) then Eq. (10) is reduced to

$$2N^2 E_{cond}^{exp} \approx E_{cond} \approx E_{el}^{c,SC}, \quad (11)$$

where the experimental condensation energy E_{cond}^{exp} is usually given per unit cell, therefore the factor of $2N^2$ is employed in order to compare with the calculated E_{cond} for the superlattice of the coherence area. Further studies will be needed, however, to understand the effect of $E_{el}^{c,NS}$ on Eq. (10).

The energy gain in the SC state is provided by the change in the inter-layer charging energy which is essentially the change of the out-of-plane hole-anti-hole interaction energy below T_c . *However, the hole-conductivity in the SC state is strictly 2D phenomenon, no direct IL hopping of quasiparticles is considered within this model.* T_c is mainly determined by the inter-plane distance and by the static *c*-axis dielectric constant (the *c*-axis component of the dielectric tensor). *An interesting feature of the $N \times N$ bilayer model is then that it is capable of retaining the 2D character of SC while T_c is enhanced by 3D Coulomb interactions.*

IV. THE DIELECTRIC CONSTANT ϵ_c WITHIN THE BCS LIMIT

The model outlined in the previous section allows us to estimate the static dielectric constant ϵ_c for various cuprates. First we give the brief derivation of the formula starting from the BCS equation for the gap [17],

$$k_{BCS} k_B T_c = \Delta(0), \quad (12)$$

where k_B is the Boltzman constant and the gap ratio $k_{BCS} \approx 3.53$ for normal superconductors at weak-coupling limit [17]. The BCS estimate of the condensation energy (the energy gain in the SC state) is proportional, however to $\sim \Delta_g^2$, therefore we can use the following expression [17],

$$E_{cond} = -\frac{1}{2} N(0) \Delta(0)^2 = -\frac{1}{2} N(0) k_{BCS}^2 k_B^2 T_c^2, \quad (13)$$

where $N(0)$ is the density of states at the Fermi surface [17]. We recall now Eq. (11),

$$E_{cond} \approx E_{el}^c = \frac{e^2}{4\pi\epsilon_0\epsilon_c} \sum_{n=1}^2 \sum_{m=2}^{\infty} \sum_{ij} \frac{q_i^{(n)} q_j^{(m)}}{r_{ij}^{(n,m)}}, \quad (14)$$

from which ϵ_c can be derived,

$$\epsilon_c \approx \frac{e^2}{4\pi\epsilon_0 E_{cond}} \sum_{n=1}^2 \sum_{m=2}^{\infty} \sum_{ij} \frac{q_i^{(n)} q_j^{(m)}}{r_{ij}^{(n,m)}}. \quad (15)$$

Using Eq. (13) E_{cond} can be substituted into Eq. (15) leading to a new expression,

$$\epsilon_c = \frac{2e^2}{4\pi\epsilon_0 N(0)k_{BCS}^2 k_B^2 T_c^2} \sum_{n=1}^2 \sum_{m=2}^{\infty} \sum_{ij}^{2N^2} \frac{q_i^{(n)} q_j^{(m)}}{r_{ij}^{(n,m)}}. \quad (16)$$

$N(0)$ can be obtained from first-principles calculations or from specific-heat measurements. $N(0)$ is connected with the Sommerfeld constant γ in the low-temperature electronic specific heat by the relation

$$N(0) = \gamma [2 \frac{\pi^2}{3} k_B^2 (1 + \lambda)]^{-1}, \quad (17)$$

λ is a coupling constant due to strong electron-phonon renormalization. γ can be obtained from specific heat measurements [2]

$$1.43\gamma = \Delta C/T_c, \quad (18)$$

where γ is usually given in $[mJ/mol.K^2]$ therefore $\sim 2N^2\gamma$ must be used for the coherence area of $\sim \xi_{ab}^2$ (twice for the bilayer). Finally we get the expression for the static c -axis dielectric constant

$$\epsilon_c = \frac{\pi e^2 (1 + \lambda)}{6\epsilon_0 k_{BCS}^2 N^2 \gamma T_c^2} \sum_{n=1}^2 \sum_{m=2}^{\infty} \sum_{ij}^{2N^2} \frac{q_i^{(n)} q_j^{(m)}}{r_{ij}^{(n,m)}}. \quad (19)$$

The only unknown parameter in Eq. (19) is λ which is in the range of $\lambda = 1 - 2$ when strong electron-phonon coupling is assumed [2].

V. BEYOND THE BCS LIMIT

There are number of evidences are available which suggest that HTSC occurs beyond the BCS limit. In those materials which contain nearly isolated single layers, such as $Bi_2Ba_2CuO_{6+\delta}$ [50] or superlattice structures (periodic artificially layered materials) such as O-doped $(BaCuO_2)_2/(CaCuO_2)_n$ thin films, when $n = 1$ [54] and in $YBa_2Cu_3O_{7-\delta}/PrBa_2Cu_3O_{7-\delta}$ [2,51] the critical temperature is limited to $T_c \leq 30K$ (below the BCS limit). Therefore it is worth to explain the enhancement of T_c beyond the BCS limit assuming other mechanism than the electron-phonon coupling. Inter-layer Coulomb coupling can be a natural source of the condensation energy and of HTSC. Assuming that thermal equilibrium occurs at T_c for the competing phases of the NS and the SC state the following equation for the condensation energy can be formulated:

$$2N^2 E_{cond}^{exp} \approx k_B T_c \approx E_{el}^{c,SC} \quad (20)$$

This expression leads to the very simple formula for the critical temperature

$$T_c(N, dq, d, \epsilon_c) \approx \frac{e^2}{4\pi\epsilon_0\epsilon_c k_B} \sum_{n=1}^2 \sum_{m=2}^{N_l} \sum_{ij}^{2N^2} \frac{q_i^{(n)} q_j^{(m)}}{r_{ij}^{(n,m)}} \quad (21)$$

where N_l is the number of layers along the c -axis. When $N_l \rightarrow \infty$, bulk T_c is calculated. T_c can also be calculated for thin films when N_l is finite. and ϵ_c can also be derived

$$\epsilon_c \approx \frac{e^2}{4\pi\epsilon_0 k_B T_c} \sum_{n=1}^2 \sum_{m=2}^{N_l} \sum_{ij}^{2N^2} \frac{q_i^{(n)} q_j^{(m)}}{r_{ij}^{(n,m)}}, \quad (22)$$

where a c -axis average of ϵ_c is computed when $N_l \rightarrow \infty$. Within this picture the IL interaction energy of the charge ordered condensate in the SC state is available as condensation energy. It is not necessary, however, to assume that $E_{el}^{c,SC}$ is available as pair-binding energy, simply the superconducting phase is stabilized *vs.* the NS due to $E_{el}^{c,SC}$. Therefore $E_{cond}^{HTSC} \approx k_B T_c$ holds because of thermodynamic reasons and not because of the microscopic mechanism of pairing.

In order to test the validity of our approach we estimate the *condensation energy* and compare with the measured value. According to Tsvetkov *et al.* $E_{cond}^{exp} = 3.7 \cdot 10^{-6}$ Hartree/unit cell ($\sim 100\mu eV/Cu$) for $Tl_2Ba_2CuO_6$ ($T_c = 85K$) [14]. For the bilayer 5×5 model we have $50E_{cond}^{exp} \approx 0.19mH$ ($2N^2 = 50$) which is really comparable with $k_B T_c = 0.27mH$. The 6×6 lattice would give relatively small $\epsilon_c = 2.6$, however $72E_{cond}^{exp} \approx 0.27mH$ is in agreement with $k_B T_c$. In the case of YBCO ($YBa_2Cu_3O_7$) the $N = 4$ lattice accounts for the measured condensation energy ($\sim 3K/u.c.$) [37] the best: $2N^2 \times 3K = 96K$ which is fairly close to $T_c = 93K$. The generally quoted $\xi_{ab} \approx 15\text{\AA}$ [17,38] is indeed in accordance, with the 4×4 to 5×5 coherence area.

VI. THE CALCULATED DIELECTRIC CONSTANT

In Table I. we have calculated the static dielectric function ϵ_c using Eqs. (19) and (22).

It must be noted that experimental measurement of ϵ_c in cuprates is often troublesome. Different studies often lead to different values due to the inaccuracy provided by reflectance or conductivity measurements. Measurements on polycrystalline samples of $Bi_2Sr_2RCu_2O_8$ ($R = Sm, Y$) provided ϵ_c as large as 10^4 at 300 K [43]. Also, other studies indicate large ϵ_c in the parent insulators of HTSCs [43]. It is even more difficult to accurately measure ϵ_c for a SC sample [43]. In other studies also large ϵ_c values have been reported for $YBa_2Cu_3O_{6+\delta}$ and extremely large for the non-superconducting $PrBa_2Cu_3O_{6+\delta}$ [44,45]. Tsvetkov *et al.* reported the value of $\epsilon_c = 11.3$ for Tl2201 using optical measurements [14]. ϵ_c can be extracted from the c -axis optical measurements using the relation [14,37]

$$\sqrt{\epsilon_c} = \frac{c}{\omega_p \lambda_c}, \quad (23)$$

where c , ω_p and λ_c are the speed of light, c -axis plasma frequency and the c -axis penetration depth. In other

TABLE I. Calculated dielectric constant ϵ_c using Eqs (19) and (22) in the single-layer cuprates.

	$d(\text{\AA})$	$T_c(K)$	N	$\epsilon_c/\text{Eq. (19)}$	$\epsilon_c/\text{Eq. (22)}$	ϵ_c^{exp}
CaCuO ₂ ^a	4.64	89	5	147.9	100.0	
CaCuO ₂ ^b	4.64	110	5	96.7	80.8	
CaCuO ₂	3.19	89	8	123.5	83.5	
LSCO	6.65	39	9	94.9	64.1	
			6	39.9	27.9	23 ± 3^c
			7	39.2	27.3	
Hg1201	9.5	95	8	16.3	11.3	
			5	17.7	27.6	34^d
			5	15.9	27.6	
Hg- (10 GPa)	~ 8.5	$\sim 105.$	5	12.6	25.0	
			5	13.5	8.7	11.3^e
			5	41.6	26.8	
Tl2201	11.6	85	4	39.4 ^f		
			5	214.5	32.6	$\sim 40^g$
			5	729.3	110.8	
Bi2201	12.2	20	6	66.6	10.1	
			4	27.5	19.4	34^f
			5	44.1	31.1	
YBCO	8.5 ^h	93	4	21.6	20.2	
LSCO ⁱ	6.65	51.5	7			

where N is the number of lattice sites along the width of the square superlattice ($N \approx \xi_{ab}/a + 1$), dq is the charge separation in the charge ordered state, d is the inter-layer distance in \AA [9], T_c is the experimental critical temperature. ^a field effect doped material [18]. ^b $Ca_{0.3}Sr_{0.7}CuO_2$ [47], ^c [42], ^d experimental ϵ_c^{exp} values are taken from *Am Inst. of Phys. Handbook*, McGraw-Hill, Ed. D, E. Gray (1982), the ϵ_c value of the ionic-background (Hg1201: BaO, Tl2201: Tl_2O_5), The pressure dependent T_c values and IL distance date are taken from [53,55], ^e from [14], ^g from [31], ^h for YBCO the reduced IL $d = 8.5\text{\AA}$ is used instead of the c -axis lattice constant (interbilayer block distance), ^f from [52], ⁱ from [62]. The notations are as follows for the compounds: LSCO ($La_{0.85}Sr_{0.15}CuO_4$), Hg1201 ($HgBa_2CuO_{4+\delta}$), Tl2201 ($Tl_2Ba_2CuO_6$), Bi2201 ($Bi_2Sr_2CuO_6$) and YBCO (YBa_2CuO_7).

cases only the ϵ_c of certain elements of the ion-core spacer is available such as e.g. BaO in Hg1201 and in YBCO. It must be emphasized that the reported experimental ϵ_c values are frequency dependent and show relaxation behaviour therefore the comparison is not easy with our reported values. For the prototypical cuprate LSCO we get the value of $\epsilon_c = 27.3$ which is comparable with the experimental value of 23 [42] using $N = 7$ which corresponds to $6a_0 \approx 23.4\text{\AA}$ ($\xi_{ab} \approx 20 - 30\text{\AA}$ [58]).

We try to explain the doping function $T_c(\delta)$ using the $N \times N$. The coherence area ($\sim \xi_{ab}$) systematically varies with doping and reaches its minimum at optimal doping ($n_h \approx 0.16$). Therefore, the contraction of the pair-condensate wave-function $\Psi(r_1, r_2)$ is the most pronounced at optimal doping accommodated by 4×4 to 5×5 superlattice. When the system is *underdoped*, the $E_{el}^c[n_h(\delta)]$ scales almost linearly with δ . This is because the smaller $n_h(\delta)$ leads to smaller inter-layer charging energy while ϵ_c is nearly unchanged. This behaviour is

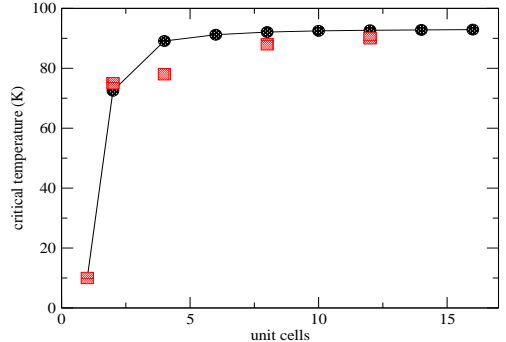


FIG. 4. The critical temperature T_c (K, Eqs. (20)-(22)) vs. the number of unit cells along the c -axis in YBCO using the 4×4 model. Circles and squares correspond to the calculated and experimental values [51].

clearly described by Eq. (21). However, in the *overdoped* regime more and more charge is confined to the inter-layer space, which increases ϵ_c , hence decreases T_c . The physical explanation is that the increased density of inter-layer hole-charge screens the dielectric medium (e.g. Ca^{2+}), which leads to less effective polarization of the condensed part of the hole charge. In the *optimally doped* materials the confinement of the hole content in the planes is the most pronounced in the SC state. Doping induced out-of-plane charge transport, such as the strong c -axis anisotropy of the hole content, leads to charge inhomogeneity, and might lead to large ϵ_c [43].

Multilayer and *pressure* effects on T_c can also be discussed in terms of in-plane and out-of-plane localization of the hole charge. In multilayer systems E_{el}^c is composed of intra- and inter-block contributions. We use the notation block for the multilayer parts $CaCu_2O_4$, $Ca_2Cu_3O_6$, etc. Eq. (11) can then be modified for multilayer cuprates as follows,

$$E_{\text{cond}} \approx E_{el}^{c,\text{intra}} + E_{el}^{c,\text{inter}}, \quad (24)$$

where

$$E_{el}^{c,\text{intra}} = (l-1)E_{el}^c(d_{\text{intra}}, \epsilon_{\text{intra}}), \quad (25)$$

l denotes the number of layers. Therefore, intra-block charging energy further enhances T_c on top of the corresponding single-layer inter-block value. YBCO is a peculiar example of cuprates in which HTSC is purely coming from *inter-block coupling* as it was explained on the basis of $YBa_2Cu_3O_{7-\delta}/PrBa_2Cu_3O_{7-\delta}$ superlattice structures [2]. In YBCO the $Y(CuO_2)_2$ bilayer alone does not show HTSC when isolated from each other in artificially layered materials ($T_c \approx 20K$). The dependence of T_c in YBCO on the number of unit cells along the c -axis is calculated using Eq. (25) and the results are depicted on FIG 4. The experimental points [51] are relatively well reproduced indicating that ~ 5 unit cell thick thin film is already the reminiscent of the bulk properties of cuprates.

It is worth mentioning the *intercalation* experiment on Bi2212 [3]. Intercalation of I or organic molecules into the $(BiO)_2(SrO)_2$ layers of Bi2212 results in no significant change in T_c . Basically inter-layer intercalation is introduced to reduce interlayer coupling (test of inter-layer theory, ILT) and to enhance anisotropy in SC properties. It was concluded that these results presents great challenge to ILT [6] and support low-dimensional SC theories. In the light of the $N \times N$ model, it is not surprising that in Bi2212 the nearly isolated bilayers are superconductors. The single layer material Bi2201 ($Bi_2Sr_2CuO_6$) gives very low T_c ($\approx 20K$) [50], which indicates that the dielectrics $(BiO)_2(SrO)_2$ strongly reduces IL coupling, indeed the estimated ϵ_c is quite large (Table I) which is attributed to the weakly interacting $(BiO)_2$ bilayer (the BiO-BiO distance is $\sim 3.7\text{\AA}$ [3]). Dielectric constant measurements [41] on Bi-compounds also provide relatively large dielectric constants in accordance with our calculations. The extremely large conduction anisotropy $\gamma \sim 10^6$ found in Bi-based cuprates also supports these findings [2]. Nearest-neighbouring Cu-O planes in Bi-compounds are nearly insulated [52]. Therefore, in the multilayer Bi-compounds bilayer and trilayer blocks are responsible for the high- T_c , inter-block coupling is negligible. The multilayer Bi-compounds provide then an example for *pure intra-block HTSC*. In these materials the multilayer-blocks are dielectrically isolated. However, in the most of the cuprates T_c is enhanced both via intra- and inter-block effects. An important consequence of the bilayer $N \times N$ model is that *isolated single layers do not show HTSC*, coupling to next-nearest CuO_2 plane is essential in HTSC. It is possible then to estimate ϵ_c for the bilayer block, since $E_{el}^{c,inter} \approx 0$ in the Bi-compounds in Eq. (24). In the hypothetical bilayer system in Table 1. ($Ca(CuO_2)_2$, $d = 3.19\text{\AA}$, $T_c = 89K$), which is the building block of multilayer cuprates, we find the value of $N = 8$ accounting for realistic ϵ_c . $N = 8$ is in accordance with the measured relatively "large" coherence length of $\xi_{ab} \approx 27\text{\AA}$ ($(N - 1)a_0 = 7a_0 \approx 27.3\text{\AA}$) [56].

Also, upon pressure (p) the inter-layer spacing decreases, which increases E_{el}^c without the increase of the hole content. Saturation of $T_c(p)$ is reached simply when increasing IL sterical repulsion starts to destabilize the system. In systems, such as YBCO or LSCO, negative or no pressure dependence of T_c is found [2] due to the short Cu-O apical distance ($d_{CuO} \approx 2.4\text{\AA}$) which leads to steric repulsion at ambient pressure and to the weakening of HTSC. In these systems the net gain in charging energy is not enough to overcome steric repulsions.

With these results, we are now in a position to reach the conclusion that the $N \times N$ model can readily account for at least certain physical properties of multilayer cuprates, such as pressure, doping and multilayer dependence of T_c . Furthermore it is possible to make some estimations on the upper limit of T_c using Eq. (22) for T_c . Assuming relatively small $\epsilon_c \approx 10$ and short inter-layer spacing $d \approx 7.0\text{\AA}$ we get the value of $T_c \approx 333K$ for a strongly localized electron pair with 5×5 coherence area.

Of course, we have no clear cut knowledge at this moment on how the pair condensate wave-function spreads upon varying ϵ_c and d . Effective localization of the Cooper-pair wave-pocket could lead, however, to room temperature superconductivity under proper structural and dielectric conditions if the model presented above is applicable.

According to the stripe scenario, the charge ordered state of the coherence area can also be seen in many cuprates as one-dimensional stripe order or charge density waves [59]. The striped antiferromagnetic order found in LSCO by magnetic neutron scattering experiments [60] also implies a spin-density of periodicity $\sim 8a$ a reminiscent of the coherence area. The incommensurate "checkerboard" patterns seen with a spatial periodicity of $\sim 8a_0$ in the vortex core of Bi2212 obtained by scanning tunneling microscopy [61] is also consistent with our $N \times N$ hole-anti-hole charge ordered state where $N = 8$ to 9 in BSSCO.

Finally we mention the recent results of Bozovic *et al.* [62] obtained for LSCO thin films under epitaxial strain. They reached the record $T_c = 51.5K$ for 15-unit-cell thick film of LSCO on $LaSrAlO_4$ substrate. The small variation of the ab - or c -axis lattice constants in our model accounts for only 1 – 2 K increase in T_c . We explain the more than 10 K enhancement of T_c with the decrease of ϵ_c (Table I.) under the conditions they used (O_3 annealing, epitaxial strain provided by the substrate).

VII. CONCLUSION

In this paper we studied the pair condensation and confinement of the hole-content on a CuO_2 superlattice layer as a function of inter-layer distance and dielectric permittivity of the charge reservoir.

- The assumption of a $2D \Leftrightarrow 3D$ quantum phase transition of the hole-content at T_c in HTSC materials is thought to be an important general feature of pair-condensation and is supported by c -axis optical measurements and by first-principles calculations. Our proposal is that the c -axis charge dynamics of the hole-content contributes significantly to the condensation energy below T_c .
- We have found that a pair condensate can be distributed on a $N \times N$ square lattice layer in such a way that the lattice sites are filled by $\pm q = [0, 0.16e]$ condensed charge alternatively depending on the hole($+q$)-anti-hole($-q$) charge separation dq . In this way a charge ordered state of the pair-condensate occurs with a "checkerboard" like pattern seen recently by experiment [61]. The phase separation of hole-electron pairs (hole-anti-hole pairs) in this model is stabilized electrostatically. The maximum charge separation is $dq = 0.32e$, if the optimal hole content $n_h \approx 0.16e$.

- In the adjacent layer the electron-hole pairs are distributed in a complementer way (charge asymmetry) in order to maximize the inter-layer charging energy. Holes on one plane are covered by anti-holes on the other, and vice versa. In this way we derived a charge ordered $N \times N$ bilayer model of the superconducting state with inter-layer charge mirror symmetry which directly leads to inter-layer Coulomb energy gain in the superconducting state.
- The superlattice nature of the pair condensate is directly related to the smallest size of the condensate wave-pocket which is remarkably comparable with the measured in-plane coherence length of $\xi_{ab} = 10 - 20 \text{ \AA}$ ($4a_0 \approx 15.6 \text{ \AA}$) of cuprates, where $a_0 \approx 3.9 \text{ \AA}$ is the in-plane lattice constant. The coherence area of the Cooper pair in cuprates is strongly localized, which is due to inter-layer charging effects.
- The bilayer model with $4e$ boson charge naturally implies the mass enhancement of $m^* \approx 4m_e$ in accordance with measurements. The experimental condensation energy obtained for Tl2201 and YBCO is also in accordance with the 4×4 to 5×5 bilayer superlattice model.
- The static dielectric constant ϵ_c is calculated for a couple of cuprates and compared with the available experimental measurements. The general agreement is quite good indicating that the pure inter-layer electrostatic model leads to proper description of the static dielectric response of these layered materials.
- The basic microscopic mechanism of HTSC is to be understood within the BCS-Eliashberg theory at low temperatures. The limiting critical temperature for BCS-type superconductor is around $20K$ as it was found for cuprates with nearly isolated CuO_2 layers (BSCCO, YBCO/PrBCO superlattices etc.). At higher temperatures up to T_c the SC phase is stabilized *vs.* the NS by the inter-layer Coulomb interaction due to the inter-layer charge antisymmetry of the pair condensate.
- We propose to understand chemical- and field-effect doping as a hole-content confinement mechanism, induced by the electrostatic field of the charged dopant atom (chemical doping) or by the external field (in a field effect transistor) below T_c .

The detailed study of this model showed that the inter-layer charging energy is proportional to the thermal motion at T_c , if the c -axis dielectric constant ϵ_c and the coherence area is appropriately chosen.

If the physical picture derived from our model is correct, it should be a guide for further experimental studies

aiming to improve SC in cuprates or in other materials. This can be done by tuning the IL distance and ϵ_c (increasing the polarizability of the dielectric, hence decreasing ϵ_c) in these materials. The application of this model to other class of HTSC materials, such as fullerides or MgB_2 is expected to be also effective.

Further development of the model presented here, such as using charge density $\rho(r)$ instead of point charges within a self-consistent quantum theory, would make it possible to study the external field or chemical doping induced c -axis charge distribution in cuprates. This is however, beyond the scope of the present article and is planned in the near future.

VIII. ACKNOWLEDGEMENT

I would like to thank for the helpful discussions with T. G. Kovács and E. Sherman. This work is supported by the OTKA grant MFA-42/2002 from the Hungarian Academy of Sciences

- [1] J. E. Hirsch, *Science* **295**, 2226. (2002)
- [2] N. M. Plakida, *High-Temperature Superconductivity*, Springer, 1995
- [3] J. Choy *et al.*, *Science* **280**, 1589. (1998), X-D. Xiang, *et al.*, *Nature* **348**, 145. (1990)
- [4] D. N. Basov *et al.*, *Science* **283**, 49. (1999)
- [5] P. W. Anderson, *The Theory of Superconductivity in the High- T_c Cuprate Superconductors*, Princeton Univ. Press, 1997
- [6] P. W. Anderson, *Physica* **C341-348**, 9. (2000), *cond-mat/0201429*
- [7] T. Schneider, *condmat/0110173*, T. Schneider, H. Keller, *Phys. Rev. Lett.* **86**, 4899. (2001)
- [8] J. M. Wheatley, T. C. Hsu, P. W. Anderson, *Nature* **333**, 121. (1988)
- [9] D. R. Harshman, A. P. Mills, *Phys. Rev.* **B45**, 10684. (1992), and references therein
- [10] Z. Tesanovic, *Phys. Rev.* **B36**, 2364. (1987)
- [11] A. K. Rajagopal, S. D. Mahanti, *Phys. Rev.* **B44**, 10210. (1991), S. S. Jha, A. K. Rajagopal, *Phys. Rev.* **B55**, 15248. (1997)
- [12] X.-D. Xiang, *et al.*, *Phys. Rev. Lett.* **68**, 530. (1992)
- [13] J. Ihm and B. D. Yu, *Phys. Rev.* **B39**, 4760. (1989)
- [14] A. A. Tsvetkov *et al.*, *Nature*, **395**, 360. (1998)
- [15] H. J. A. Molegraaf, C. Presura, D. van der Marel, P. H. Kes, M. Li, *Science* **295**, 2239. (2002), D. van der Marel, A. Tsvetkov, M. Grueninger, H. J. A. Molegraaf, *Physica* **C341-348**, 1531. (2000)
- [16] J. E. Hirsch, *Physica* **C199**, 305. (1992)
- [17] M. Tinkham, *Introduction to Superconductivity*, McGraw-Hill, Inc. New York, 1996

- [18] J. H. Schön, *et al.*, *Nature* **414**, 434. (2001)
- [19] H. Zhang and H. Sato, *Phys. Rev. Lett.* **70**, 1697. (1993)
- [20] K. Tamasku, Y. Nakamura, S. Uchida, *Phys. Rev. Lett.* **69**, 1455. (1992)
- [21] S. Tajima, *et al.*, *Phys. Rev.* **B48**, 16164. (1993)
- [22] A. S. Katz, *et al.*, *Phys. Rev.* **B61**, 5930. (2000)
- [23] D. N. Basov, *et al.*, *Phys. Rev.* **B63**, 134514. (2001)
- [24] T. Motohashi, *et al.*, *Phys. Rev.* **B61**, 9269. (2000)
- [25] W. E. Pickett, *Rev. Mod. Phys.* **61**, 433. (1989)
- [26] R. P. Gupta, M. Gupta, *Phys. Rev.* **B21**, 15617. (1995)
- [27] P. Süle, C. Ambrosch-Draxl, H. Auer, E. Y. Sherman, *cond-mat/0109089*
- [28] Y. Ando, A. N. Lavrov, S. Komiya, K. Segawa, X. F. Sun, *condmat/0104163*
- [29] K. Semba, A. Matsuda, *Phys. Rev. Lett.* **86**, 496. (2001)
- [30] A. Yamamoto, W. Hu, S. Tajima, *Phys. Rev.* **B63**, 24504. (2001)
- [31] H. Kitano, T. Hanaguri, A. Maeda, *Phys. Rev.* **B57**, 10946. (1998)
- [32] T. Fujii, *et al.*, *cond-mat/0205121*, L. He, *et al.*, *cond-mat/0110166*, W. Si, *et al.*, *cond-mat/0205153*
- [33] R. Friedberg, H. S. Zhao, *Phys. Rev.* **B44**, 2297. (1991), *Phys. Rev.* **B39**, 11482. (1989)
- [34] E. Dagotto, *Rev. Mod. Phys.* **66**, 763. (1994)
- [35] S. Stinzen, Z. Zwebger, *Phys. Rev.* **B56**, 9004. (1997)
- [36] M. Di Stasio, K. A. Müller, L. Pietronero, *Phys. Rev. Lett.* **64**, 2827. (1990), and references therein
- [37] P. W. Anderson, *Science*, **279**, 1196. (1998)
- [38] U. Welp, *et al.*, *Phys. Rev. Lett.* **62**, 1908. (1989)
- [39] L. Krusin-Elbaum *et al.*, *Phys. Rev. Lett.* **62**, 217. (1989)
- [40] C. Kittel, *Quantum Theory of Solids*, Wiley & Sons, New York, (1987)
- [41] K. B. R. Varma, *et al.*, *Appl. Phys. Lett.* **55**, 75. (1989)
- [42] Optical reflectance measurements indicate an in-plane dielectric constant of 5-6 at low frequencies: D. Reagor *et al.*, *Phys. Rev. Lett.* **62**, 2048. (1989)
- [43] T. Takayanagi, M. Kogure, I. Terasaki, *cond-mat/0108483*, and references therein, I. Terasaki, T. Mizuno, K. Inagaki, Y. Yoshino, *condmat/0204537*
- [44] C. M. Rey, *et al.*, *Phys. Rev.* **B45**, 10639. (1992)
- [45] G. P. Mazzara, *et al.*, *Phys. Rev.* **B47**, 8119. (1993)
- [46] R. M. Hazen, *Crystal Structures of High Temperature Superconductors*, in *Physical Properties of High Temperature Superconductors*, Ed. D. M. Ginsberg, (1990)
- [47] M. Azuma *et al.*, *Nature (London)* **356**, 775. (1992)
- [48] J. R. Kirtley, *et al.*, *Phys. Rev. Lett.* **81**, 2140. (1998)
- [49] P. Nozières, D. Pines, *The Theory of Quantum Liquids*, Perseus Books, 1999
- [50] Z. Konstantinović, *et al.*, *Phys. Rev.* **B66**, 20503. (2002)
- [51] Q. Li, *et al.*, *Phys. Rev. Lett.* **64**, 3086. (1990)
- [52] D. Ariosa, H. Beck, *Phys. Rev.* **B43**, 344. (1991)
- [53] D. L. Novikov *et al.*, *Phys. Rev.* **B54**, 1313. (1996)
- [54] G. Balestrino *et al.*, *Phys. Rev.* **B58**, 8925. (1998)
- [55] L. Gao, *et al.*, *Phys. Rev.* **B50**, 4260. (1994)
- [56] I. Matsubara, *et al.*, *Phys. Rev.* **B45**, 7414. (1992)
- [57] R. Kleiner, *et al.*, *Phys. Rev. Lett.* **68**, 2394. (1992)
- [58] See e.g. *Physical Properties of High Temperature Superconductors*, Ed. D. M. Ginsberg, (1989)
- [59] C. Howald, *et al.*, *cond-mat/0208442*
- [60] B. Lake, *et al.*, *Nature* **415**, 299. (2002)
- [61] J. E. Hoffman *et al.*, *Science* **295**, 466. (2002)
- [62] I. Bozovic *et al.*, *Phys. Rev. Lett.* **89**, 107001. (2002)